# Tetrahedral Element Shape Optimization via the Jacobian Determinant and Condition Number

Lori A. Freitag
Mathematics and Computer Science Division
Argonne National Laboratory
Argonne, IL 60439
freitag@mcs.anl.gov

Patrick M. Knupp
Parallel Computing Sciences Department
Sandia National Laboratories
M/S 0441, P.O. Box 5800
Albuquerque, NM 87185-0441
pknupp@sandia.gov

**Abstract.** We present a new shape measure for tetrahedral elements that is optimal in the sense that it gives the distance of a tetrahedron from the set of inverted elements. This measure is constructed from the condition number of the linear transformation between a unit equilateral tetrahedron and any tetrahedron with positive volume. We use this shape measure to formulate two optimization objective functions that are differentiated by their goal: the first seeks to improve the average quality of the tetrahedral mesh; the second aims to improve the worst-quality element in the mesh. Because the element condition number is not defined for tetrahedra with negative volume, these objective functions can be used only when the initial mesh is valid. Therefore, we formulate a third objective function using the determinant of the element Jacobian that is suitable for mesh untangling. We review the optimization techniques used with each objective function and present experimental results that demonstrate the effectiveness of the mesh improvement and untangling methods. We show that a combined optimization approach that uses both condition number objective functions obtains the best-quality meshes.

**Keywords.** Mesh Improvement, Optimization-based Mesh Smoothing, Mesh Quality, Mesh Untangling

## 1 Introduction

Local mesh smoothing algorithms are commonly used for simplicial mesh improvement. These methods relocate a set of adjustable vertices, one at a time, to improve mesh quality in a neighborhood of that vertex. The new grid point position is determined by considering a local submesh containing the adjustable, or *free vertex*, $v$, and its incident vertices and elements. For example, in Figure 1, we show a two-dimensional local submesh with three possible locations for $v$. The leftmost local submesh shows a valid but poor-quality mesh, the middle submesh shows a higher-quality valid mesh, and the rightmost shows an invalid mesh with inverted elements. Overall improvement in the mesh is obtained by performing some number of sweeps over the set of adjustable vertices.

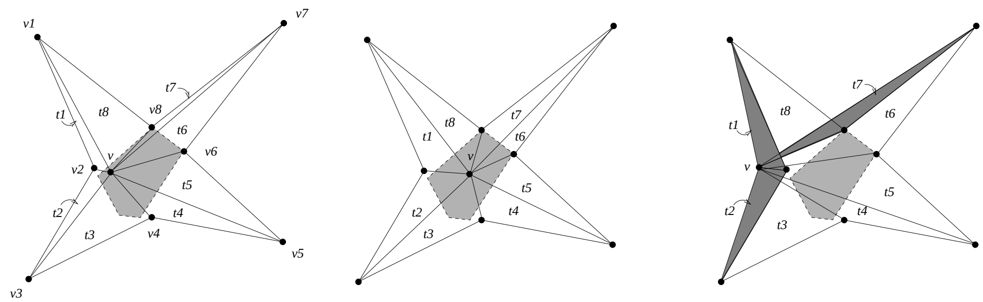


Figure 1: A local submesh with three possible locations for $v$.

The most commonly used local mesh smoothing technique is Laplacian smoothing [6, 16] which moves the free vertex to the geometric center of its incident vertices. Laplacian smoothing is computationally inexpensive but does not guarantee improvement in the element quality.

To address this problem, several optimization-based approaches to mesh smoothing have been developed in recent years, for example, [19, 11, 1, 18, 14]. In these techniques, the local submesh is evaluated according to some objective function based on a quality metric, $q_i$, such as element angle or aspect ratio. Function and, possibly, gradient information are used to relocate the free vertex in such a way that the objective function is optimized. For example, if the quality metric under consideration is element angle, the leftmost submesh in Figure 1 shows an initial position for $v$ that results in three poor-quality elements, $t1$, $t2$, and $t7$. The middle submesh in Figure 1 shows the position of $v$ that optimizes the element angle. We note that if the initial mesh contains inverted elements, objective functions that work well for mesh quality improvement may not be appropriate for mesh untangling [10].

Several optimization objective functions based on geometric criteria have been proposed for *a priori* improvement of a simplicial mesh. For example, Bank proposed a ratio of triangle area to edge length squared for two-dimensional meshes [2], Shephard and Georges proposed a similar ratio of volume to face areas for tetrahedral meshes [19], Freitag et al. used angle-based measures for both two- and three-dimensional meshes [9, 11], and Knupp has proposed a number of shape quality measures derived from simplicial element Jacobian matrices [14, 15]. Canann et al. proposed a distortion metric for both triangles and quadrilaterals that could be used with both valid and inverted elements [18]. In addition, *a posteriori* metrics have been proposed to improve finite element meshes by optimizing solution error indicators [1].

In Section 2, we propose a new shape quality metric constructed from the element condition number for the *a priori* improvement of tetrahedral meshes. We introduce the Jacobian matrix, $A_i$, associated with each tetrahedral vertex and show that its determinant is invariant with respect to the vertex at which it is evaluated. The condition numbers of the Jacobian matrices can also be made invariant by introducing a weighting that gives the linear transformation from the physical tetrahedron to the logical tetrahedron. We show that this weighted condition number is a tetrahedral shape measure according to the formal definition given in [4] and that it is optimal in that it gives the distance of a tetrahedron from the set of inverted elements.

In Section 3, we formulate two optimization objective functions using the element condition number that are suitable for mesh improvement if the initial mesh is valid. The first objective function targets the improvement of average element quality; the second targets the improvement of the worst element quality. If the initial mesh is not valid, this shape measure cannot be used for mesh improvement as it is not defined for inverted elements. In this case we use an objective function based on the determinant of the Jacobian that is suitable for untangling the inverted elements. In previous papers, we have independently proposed optimization techniques for mesh untangling [10], mesh improvement as measured by average element quality [14], and mesh improvement as measured by extremal element quality [11], and we review these optimization techniques in Section 3.2.

In Section 4, we present numerical results for each of the mesh improvement strategies using the condition number shape measure on four tetrahedral meshes.

We compare each technique to a baseline Laplacian smoother, and illustrate that in each test case, a combined optimization approach produces the best-quality meshes. We also show that the techniques can achieve high-quality meshes even when starting with an invalid mesh, by combining the mesh improvement strategies with the mesh untangling approach. Finally, in Section 5, we offer concluding remarks and directions for future research.

## 2 Tetrahedral Jacobian Matrices and Condition Numbers

In this section we discuss the Jacobian matrices associated with tetrahedral elements. We show that the Jacobian determinants are invariant for each element and that a new tetrahedral shape measure can be constructed from the Jacobian matrix condition number. The measure is optimal in the sense that it measures the distance of a given tetrahedron to the set of inverted tetrahedra.

### 2.1 Tetrahedral Jacobian Matrices

Let $T$ be an arbitrary tetrahedral element consisting of four vertices $v_n$, $n = 0, 1, 2, 3$ with coordinates $\mathbf{x}_n \in R^3$. Let $\mathcal{V}(T)$ denote the volume of the tetrahedron. Define edge vectors $e_{k,n} = \mathbf{x}_k - \mathbf{x}_n$ with $k \neq n$ and $k = 0, 1, 2, 3$ (note that $e_{n,k} = -e_{k,n}$). Vertex $v_n$ has three attached edge vectors, $e_{n+1,n}$, $e_{n+2,n}$, and $e_{n+3,n}$, where the indices are taken modulo four. Define the Jacobian matrix at node $n$ (denoted by $A_n$) to consist of the columns of the triplet of attached edge vectors, namely,

$$A_n = (-1)^n \begin{pmatrix} e_{n+1,n} & e_{n+2,n} & e_{n+3,n} \end{pmatrix}.$$

Let $\alpha_n$ be the determinant of $A_n$.

**Theorem 1**. The determinants $\alpha_n = \alpha_0$ for $n = 1, 2, 3$.
**Proof**.
Let M be the following constant matrix

$$M = \begin{pmatrix} 1 & 1 & 1 \\ -1 & 0 & 0 \\ 0 & -1 & 0 \end{pmatrix}.$$

The determinant of M equals 1. A direct calculation shows that

$$A_n = A_0 \, M^n$$

for $n = 1, 2, 3$. Taking the determinant of this expression gives $\alpha_n = \alpha_0$. §

It is well known that the volume of a tetrahedron is one-sixth of the Jacobian determinant [12], hence $\alpha_0 = 6\,\mathcal{V}(T)$ and $\mathcal{V}(T) > 0$ if and only if $\alpha_0 > 0$. An element is said to be *invertible* if and only if $\alpha_0 > 0$.

Matrix norms are a critical part of the theory to be presented. Let $I$ be the identity matrix and $S$ be an arbitrary matrix. The Euclidean norm of $S$ is defined in terms of the trace:

$$| S | = [\, tr(S^T S) \,]^{1/2}.$$

The Euclidean norm is invariant to rotation matrices, that is, $| SR | = | RS | = | S |$, where R is a rotation matrix ($R^T R = I$, $| det(R) | = 1$). If $S$ is invertible, then $S^{-1}$ exists, and one can define the adjoint matrix of $S$:

$$adj\,(S) = \sigma \, S^{-1},$$

where $\sigma = det(S)$.

One can easily show that the following relationships hold for the Jacobian matrix:

$$\begin{aligned} | A_n |^2 &= | e_{n+1,n} |^2 + | e_{n+2,n} |^2 + \\ &\quad\; | e_{n+3,n} |^2, \text{ and} \\ | adj\,(A_n) |^2 &= | e_{n+1,n} \times e_{n+2,n} |^2 + \\ &\quad\; | e_{n+2,n} \times e_{n+3,n} |^2 + \\ &\quad\; | e_{n+3,n} \times e_{n+1,n} |^2 . \end{aligned}$$

These provide a geometric interpretation of the norms. The norm-squared of $A_n$ is the sum of the lengths-squared of the attached edge vectors and the norm-squared of the adjoint is the sum of the squares of the areas of the attached triangular faces.

Unlike the determinant, $\alpha_n$, the norms of $A_n$ and $adj\,(A_n)$ are not independent of $n$ because not all of the lengths and areas of the tetrahedron affect the result for $A_n$. This situation can be remedied, as will be shown next.

Define an equilateral tetrahedron $T_e$ to have sides of length one and four vertices with the coordinates $(0, 0, 0)$, $(1, 0, 0)$, $(1/2, \sqrt{3}/2, 0)$, and $(1/2, \sqrt{3}/6, \sqrt{2}/\sqrt{3})$. This tetrahedron serves as the logical element. Let $W_n$ be the Jacobian matrix at the $n$th vertex of $T_e$. For example,

$$W_0 = \begin{pmatrix} 1 & 1/2 & 1/2 \\ 0 & \sqrt{3}/2 & \sqrt{3}/6 \\ 0 & 0 & \sqrt{2}/\sqrt{3} \end{pmatrix}$$

and $w_0 = det(W_0) = \sqrt{2}/2$.

**Theorem 2.**
Let $T$ be any tetrahedron, with Jacobian matrices $A_n$. Let $S_n$ be the linear transformation that takes $W_n$ to $A_n$. Then $S_n = A_0\, W_0^{-1}$, that is, $S_n$ is independent of $n$.
**Proof.**
By definition, $S_n W_n = A_n$. If $n = 0$, $S_0 = A_0\, W_0^{-1}$. Theorem 1 applies to the matrices $W_n$ of $T_e$. Thus $W_n = W_0\, M^n$ for $n = 1, 2, 3$. Since $A_n = A_0\, M^n$, we have the stated result. §
In other words, there exists a unique linear transformation between the logical tetrahedron $T_e$ and the physical tetrahedron $T$. Because of this result, let us denote $W_0$ by $W$ and $w_0$ by $w$.

**Theorem 3.**
$\mid A_n W^{-1} \mid = \mid A_0 W^{-1} \mid$ and $\mid W A_n^{-1} \mid = \mid W A_0^{-1} \mid$.
**Proof.**
The result for $n = 0$ is immediate. Define the matrix $R = WMW^{-1}$, where $M$ is defined in the proof of Theorem 1. A direct calculation shows that $R$ is a rotation matrix with a positive determinant. Therefore, $det(R^n) = 1$ and $(R^n)^T\, R^n = I$ for $n = 1, 2, 3$; that is, $R^n$ is a rotation matrix. Hence

$$\begin{aligned} \mid A_n W^{-1} \mid &= \mid A_0 M^n W^{-1} \mid \\ &= \mid A_0 W^{-1} R^n \mid \\ &= \mid A_0 W^{-1} \mid . \end{aligned}$$

Similarly, the second result can be proved by observing that $W A_n^{-1} = (A_n\, W^{-1})^{-1} = (R^n)^{-1}\, W A_0^{-1}$ and showing that $(R^n)^{-1}$ is a rotation matrix. §
This theorem shows that the norms $\mid A_n W^{-1} \mid$ and $\mid W A_n^{-1} \mid$ are independent of $n$.

## 2.2 Tetrahedral Condition Numbers

Let $T_+$ be any tetrahedron with positive volume. Then $A_n^{-1}$ exists, and one can compute the weighted *condition number* of the matrix $A_n$

$$\kappa_w(A_n) = \mid A_n W^{-1} \mid \mid (A_n W^{-1})^{-1} \mid .$$

Since $(A_n W^{-1})^{-1} = W A_n^{-1}$, Theorem 3 shows that $\kappa_w(A_n)$ is independent of $n$. This is not true for the unweighted condition number $\kappa(A_n) = \mid A_n \mid \mid A_n^{-1} \mid$. Now let $A$ be any of the four Jacobian matrices of an invertible tetrahedron. Let $\kappa_w(A) = \mid AW^{-1} \mid \mid WA^{-1} \mid$. Recall that S is the linear transformation taking $T_e$ to $T_+$; hence $\kappa_w(A) = \mid S \mid \mid S^{-1} \mid = \kappa(S)$. That is, $\kappa(S)$ *measures the condition number of the linear transformation between the logical and physical tetrahedra.*

**Theorem 4.**
Let S be derived from a tetrahedron with positive volume. Then $3/\kappa(S)$ is a tetrahedral shape measure.
**Proof.**
We use the formal definition given in [4] to prove this assertion.

First, it is clear that $\mid S \mid$ is a continuous function of the coordinates of $T_+$, and likewise so is $\mid S^{-1} \mid$. Therefore $\kappa(S)$ is a continuous function of the coordinates of any tetrahedron with positive volume.

Second, the Jacobian matrix is invariant to translations so $\kappa(S)$ is invariant to translations. Let $\tilde{A} = \lambda\, R A$ with $\lambda > 0$ and $R$ be a rotation matrix corresponding to a uniform scaling and rotation of the tetrahedron. Let $\tilde{S} = \tilde{A}W^{-1}$. Since the Euclidean norm is invariant under rotations, it is clear that $\kappa(\tilde{S}) = \kappa(S)$.

Third, it is clear that $0 < 3/\kappa(S)$. Apply the Polar Decomposition Theorem [13] to $S$. Then there exist a rotation matrix $R$ and a symmetric, positive definite matrix $U$ such that $S = RU$. Let $\lambda_i$, $i = 1, 2, 3$, be the eigenvalues of $U$. The eigenvalues are real and positive. Then $\kappa(S) = \mid U \mid \mid U^{-1} \mid$. One can show that $\mid U \mid^2 = \lambda_1^2 + \lambda_2^2 + \lambda_3^2$, so

$$\kappa^2 = \sum_{i,j} (\lambda_i/\lambda_j)^2 .$$

This is a continuous function of three variables and its minimum may be found by computing the solution to $\partial\kappa^2/\lambda_i = 0$ with $i = 1, 2, 3$. The solution is $\lambda_i = \lambda$ where $\lambda$ is any positive constant. Hence $\kappa \geq 3$. This shows that $0 < 3/\kappa \leq 1$, as required for a tetrahedral shape measure.

Fourth, suppose $3/\kappa = 1$. Then the eigenvalues of $U$ must be constant and $U = \lambda\, I$. Then the Jacobian matrix associated with the tetrahedron must have the form $A = \lambda\, R\, W$, in other words, $3/\kappa$ attains its maximum value only if the tetrahedral element is a rotation and uniform scaling of the logical tetrahedron. The converse is easy to show.

Fifth, the definition of a degenerate tetrahedral element given in [4] is somewhat vague. As noted, a tetrahedron with a small volume is not necessarily degenerate. This is reflected in the properties of the condition number. For example, if $A = \epsilon W$, where $0 < \epsilon << 1$, then $\alpha = \epsilon^3\, det(W)$ is small, but $3/\kappa_w(\epsilon W) = 1$. Thus a tetrahedron with small volume does not necessarily make $3/\kappa(S)$ large. Reference [4] gives an example of a degenerate tetrahedron, one whose volume goes to zero but at least some of the lengths do not. Suppose there exist constants $b$ and $c$ such that $0 < b \leq\mid S \mid$ and $0 < c \leq\mid adj\,(S) \mid$. Then both $\mid A \mid$ and $\mid adj(A) \mid$ are bounded below by a positive constant. Since

$$\kappa(S) =\mid S \mid \mid adj(S) \mid / \sigma\,,$$

the limit of $3/\kappa(S)$ as $\alpha \to 0$ is zero. Hence, the condition number satisfies the requirement that a shape measure go to zero for a degenerate element, at least for the given example. The second author reported numerical experiments in [15] like those described in [17] which show that the common tetrahedral shape degeneries can be detected by the condtion number. In fact, the condition number provides a rigorous definition of a degenerate element. Let $0 < \epsilon << 1$ be given. Then $T_+$ is degnerate if $3/\kappa(S) < \epsilon$. §

It is possible to show that at least some of the other weighted nondimensional objective functions given in [15] are also tetrahedral shape measures. The distinguishing feature between the condition number and these other measures is given in the following well-known theorem [3] adapted to our current setting.

**Theorem 5**.
$1/\kappa(S)$ is the greatest lower bound for the distance of S to the set of singular matrices.
**Proof**.
Let $S$ and $X$ be $3 \times 3$ matrices with $S$ non-singular and $S + X$ singular. Write $S + X = S(I + S^{-1}X)$. If $\mid S^{-1}X \mid< 1$, then $I + S^{-1}X$ is nonsingular. This would mean that $S + X$ is nonsingular, so we must have $\mid S^{-1}X \mid\geq 1$. But $1 \leq\mid S^{-1}X \mid\leq\mid S^{-1} \mid \mid X \mid$; hence $\mid X \mid / \mid S \mid\geq 1/\kappa(S)$. Therefore

$$\min\{\mid X \mid / \mid S \mid : S + X \text{ singular}\} = 1/\kappa(S).$$

§

Since $S$ is singular if and only if $A$ is singular, we are guaranteed that minimization of $\kappa(S)$ will increase the distance between $A$ and the set of singular matrices.

Results similar to those presented in this section can be given for triangular elements.

## 3 Optimization-based Smoothing Techniques

We derive two objective functions using the element condition number that are useful for optimization-based mesh improvement. We also derive an objective function based on the determinant of the Jacobian that is useful for mesh untangling. We then briefly describe the three algorithms used for optimizing the objective functions. In each case we give references to previously published work for more detailed descriptions.

### 3.1 Optimization Objective Functions

To build objective functions for mesh improvement based on the condition number of the tetrahedron, consider a node in the interior of a valid tetrahedral mesh with $M$ attached tetrahedra. Let $A_m$ be the Jacobian matrix corresponding to the $m$th element and $S_m = A_m W^{-1}$. Let $\kappa_m = \kappa(S_m)$, $m = 0, 1, ..., M-1$ be the weighted condition number of the $m$th attached tetrahedron normalized so that an equilateral tetrahedra has a $\kappa$ value of one, and $K = (\kappa_0, \kappa_1, ..., \kappa_{M-1})$. The vector $p$-norm of $K$ can be used to construct a local objective function to minimize the condition number

$$\mid K \mid_p = [\sum_{m=0}^{M-1} \kappa_m^p]^{1/p}.$$

The choice $p = 2$ gives the $\ell_2$ norm of $K$

$$\mid K \mid_2 = [\sum_{m=0}^{M-1} \kappa_m^2]^{1/2}, \tag{1}$$

which can be used to minimize the average condition number, while $p \to \infty$ gives the $\ell_\infty$ norm

$$\mid K \mid_\infty = max_m\,\{\kappa_m,\} \tag{2}$$

which can be used to minimize the maximum condition number. For the results presented in Section 4, we reformulate the objective function as the equivalent maximization problem as follows:

$$K_{min} = min_m\,\{-\kappa_m\}. \tag{3}$$

Because the condition number is defined only for tetrahedra with positive volume, a different objective function must be used for mesh untangling. Let

$\alpha_m$, $m = 0, 1, ..., M-1$ be the Jacobian determinant of the $m$th attached tetrahedron and $\mathcal{A} = (-\alpha_0, -\alpha_1, ..., -\alpha_{M-1})$. Because $\alpha_m$ corresponds to the volume of tetrahedron $m$, we can use the following to create an objective function suitable for mesh untangling:

$$\mathcal{A}_{max} = max_m \{-\alpha_m\}.$$

As with the $\ell_{inf}$ objective function, we can reformulate this into an objective function for the equivalent maximization problem using $\alpha_m$ rather than $-\alpha_m$:

$$\mathcal{A}_{min} = min_m \{\alpha_m\}. \tag{4}$$

This is the form of the objective function used for the results presented in Section 4.

We note that some optimization techniques require the gradient of the condition number $\kappa(S)$ with respect to the free vertex position $\mathbf{x}$. Let $S = A\, W^{-1}$, $\sigma = det(S)$. One can apply the chain rule and the formulas given in [15] to compactly write the gradient:

$$\nabla\kappa = -\frac{\partial\kappa}{\partial S}\, W^{-T}\, u$$

with $u^T = [1, 1, 1]$. An explicit calculation shows that

$$\begin{aligned} \frac{\partial\kappa}{\partial S} &= \frac{\mid S\mid^2 S}{\sigma^2\,\kappa(S)}\,[\,\mid S\mid^2\ I - S^T S\,] - \kappa(S)\,S^{-T} \\ &\quad + \mid S^{-1}\mid^2\ \frac{S}{\kappa(S)}. \end{aligned}$$

### 3.2 Optimization Procedures

We now formulate the optimization problem associated with each of the objective functions given above. In each case, the characteristics of the objective function demand different solution techniques, and we briefly describe the methods used.

**Optimization of the $\ell_2$ objective function.** The formulation of the optimization problem for the $\ell_2$ objective function given in (1) is

$$\min\ [\sum_{m=0}^{M-1} \kappa_m(\mathbf{x})^2]^{1/2}. \tag{5}$$

This objective function is smooth with continuous derivatives, and the problem can be solved with various techniques for unconstrained optimization.

For gradient-based optimization of the $\ell_2$ objective function, one can use the expression given in [15]. However, attemps to apply a gradient-based approach to the condition number objective function were unsuccessful. The difficulty may have been due to the fact that the objective function is not continuous over all of $R^3$, that is, singularities in the objective function occur when the elements have zero-volume. A more sophisticated approach may overcome the problem.

For the time being, we use a robust minimization algorithm that requires only objective function values. $M$ search directions are computed from the sum of $e_{n+1,n}$ for each of the attached tetrahedra. The objective function is then evaluated at various distances along the scaled search directions, and the node is moved to the position that provides the greatest decrease in the value of the objective function. If no decrease is found, the node is not moved. More precisely, let $x$ be the current node position. Set tolerance $\epsilon = 1^{-4}$ and stopping criteria $\tau = 1^{-5}$, $\sigma_0 = 1$, $\sigma_m = 1^{-3}$, and $flag = true$.

*while (flag)*<br>
    *flag = false*<br>
    *compute* $f(x)$<br>
    $\sigma = \sigma_0$<br>
    *while (* $\sigma > \sigma_m$ *)*<br>
        $\sigma = \sigma/8$<br>
        $x_{new} = x,\ f_{new} = 1^{20}$<br>
        *loop over M attached elements*<br>
            $\tilde{x} = (1-\sigma)\,x + (x_{n+1} + x_{n+2} + x_{n+3})/2$<br>
            *compute* $f(\tilde{x})$<br>
            *if (* $f(\tilde{x}) < f_{new}$ *)*, $f_{new} = f(\tilde{x})$, $x_{new} = \tilde{x}$<br>
        *end loop over elements*<br>
        *if (* $f - f_{new} > \epsilon \mid f \mid$ *)*<br>
            $d = \mid x - x_{new} \mid$<br>
            $x = x_{new}$<br>
            $\sigma = 0$<br>
            *if (* $d > \tau$ *), flag = true*<br>
    *end while*<br>
*end while*

**Optimization of the $\ell_{inf}$ objective function.** The optimization problem for the $\ell_{inf}$ objective function given in (3) is formulated as

$$\max\ \min_{0\le m\le M-1} -\kappa_m(\mathbf{x}),$$

where each $\kappa_m$ is a nonlinear, smooth, and continuously differentiable function of the free vertex position. Let the maximum value of the functions evaluated at $\mathbf{x}$ be called the *active value*, and the set of functions that obtain that value, the *active set*, be denoted by $\mathcal{S}(\mathbf{x})$. Because multiple elements can obtain the maximum value, the composite objective function has discontinuous partial derivatives where the active set changes from one set of functions to another set.

We solve this nonsmooth optimization problem using an analogue of the steepest descent method for smooth functions. The search direction, $\mathbf{s}$, at each step is the steepest descent direction derived from all possible convex linear combinations of the gradients in $\mathcal{S}(\mathbf{x})$. The line search subproblem along $\mathbf{s}$ is solved by predicting the points at which the active set $\mathcal{S}$ will change. These points are found by computing the intersection of the projection of a current active function in the search direction with the linear approximation of each $-\kappa_m(\mathbf{x})$ given by the first-order Taylor series approximation. The distance to the nearest intersection point from the current location gives the initial step length, $\beta$. The initial step is accepted if the actual improvement achieved by moving $v$ exceeds 90 percent of the estimated improvement or the subsequent step results in a smaller function improvement. Otherwise, $\beta$ is halved recursively until a step is accepted, or $\beta$ falls below some minimum step length tolerance. More detail on this optimization algorithm can be found in [11, 7].

**Optimization of the mesh untangling objective function.** The formulation of the optimization problem for the mesh untangling objective function given in (4) is

$$\max \min_{0 \leq m \leq M-1} \alpha_m(\mathbf{x}), \tag{6}$$

where $\alpha_m$ is a linear function of the free vertex position, $\mathbf{x}$. Thus, the solution of the optimization problem can be formulated as a linear programming problem, the details of which are given in [10].

The problem is well posed if (1) the vertices of the subproblem do not all lie in a lower-dimensional subspace than the original problem and (2) none of the vertices are co-located at the same point in space. If the problem is well posed, it is solved by using the computationally inexpensive and robust simplex method. For well posed problems, we proved that the level sets of the objective functions are convex in both two and three dimensions and, hence, the local subproblem is guaranteed to converge.

We note that optimizing $\alpha_m$ results in poor-quality meshes because the technique has no motivation to create good-quality elements. In fact, this technique can distort small equilateral elements in an effort to increase their volume. In practice, meshes untangled by this procedure often contain elements with angles as small as $10^{-3}$ degrees, and this technique must be followed by one or more of the mesh improvement techniques discussed previously.

## 4 Numerical Experiments

We now demonstrate the effectiveness of each of the optimization techniques in improving tetrahedral meshes compared with a baseline Laplacian smoother. We use four tetrahedral meshes generated by the CUBIT package [5] for duct, gear, hook, and foam geometries. These meshes are shown in Figure 2. In Table 1, we give the number of elements in each mesh, $N$, and the initial mesh quality as measured by the following metrics:

1. The number of slivers in the mesh, $N_S$, namely those with a normalized condition number greater than 3.0.
2. The average normalized condition number for all of the elements in the mesh, $\kappa_{avg}$.
3. The maximum normalized condition number of any element in the mesh, $\kappa_{max}$.
4. The average and maximum tetrahedral aspect ratio given by the sum of the edge lengths squared divided by the volume of the element, $A_{\gamma_{avg}}$ and $A_{\gamma_{max}}$, respectively [17]. This metric is reported to provide a comparison between the new condition number metric and a metric that is familiar to most readers.

Both the condition number and aspect ratio quality measures are normalized so that a value of one corresponds to an equilateral tetrahedron, and increasingly larger values correspond to increasingly distorted tetrahedra. The overall quality of each initial mesh as measured by $\kappa_{avg}$ and $A_{\gamma_{avg}}$ is quite good, but each mesh contains a number of sliver elements.

Mesh improvement results are obtained by using the CUBIT and Opt-MS [8] software packages developed at Sandia National Laboratories and Argonne National Laboratory, respectively. An interface between

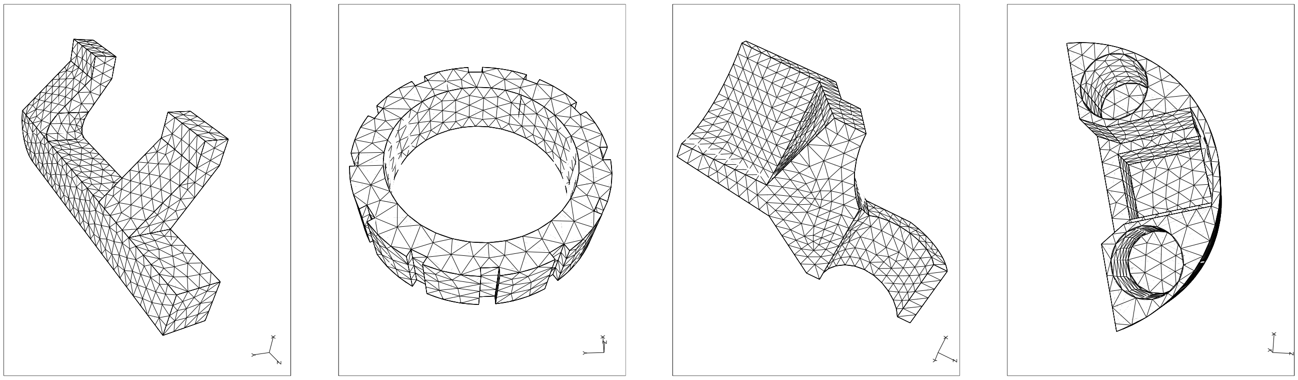

Figure 2: The four tetrahedral mesh test cases for duct, gear, hook and foam geometries

Table 1: Initial quality of the four test cases

| Geom. | $N$ | $N_S$ | $\kappa_{avg}$ | $\kappa_{max}$ | $A_{\gamma_{avg}}$ | $A_{\gamma_{max}}$ |
|---|---|---|---|---|---|---|
| Duct | 4267 | 39 | 1.305 | 3.790 | 1.441 | 5.191 |
| Gear | 3116 | 25 | 1.423 | 3.448 | 1.622 | 4.782 |
| Hook | 4675 | 30 | 1.360 | 5.176 | 1.533 | 6.151 |
| Foam | 4847 | 47 | 1.392 | 4.362 | 1.579 | 8.197 |

these two packages has been developed, and we also report the results of a combined optimization approach that uses the two software packages in concert. We will measure the success of our smoothing techniques by their ability to eliminate sliver elements and to reduce both the average and the maximum quality metric values.

### 4.1 Mesh Improvement by Condition Number Optimization

We now present results for the $\ell_2$ and $\ell_{inf}$ smoothers using the condition number objective functions described in Section 3. We attempt to improve each initial mesh described in Table 1 with six different smoothing techniques:

1. Laplacian smoothing;
2. "smart" Laplacian smoothing, which accepts a Laplacian step only if the local submesh is improved as measured by the maximum condition number;
3. $\ell_2$ smoothing as described in Section 3;
4. $\ell_{inf}$ smoothing as described in Section 3;
5. restricted $\ell_{inf}$ smoothing that is applied only if $\kappa_{max} > 3.0$ in the local submesh; and
6. a combined optimization-based approach that uses $\ell_2$ smoothing on each local submesh followed by the restricted $\ell_{inf}$ approach.

In each case, we iterate over the interior nodes in the mesh until the change in all node point positions is smaller than some tolerance.

In Table 2 we report the results of each technique in terms of the number of slivers remaining in the mesh after smoothing, the values of the quality metrics, $q_i = \kappa_{avg}$, $\kappa_{max}$, $A_{\gamma_{avg}}$, $A_{\gamma_{max}}$, as well as the percentage change from the initial value as computed by the formula

$$\mathcal{P}_i = \frac{q_{i_{final}} - q_{i_{initial}}}{q_{i_{initial}}} \times 100.$$

Because of the way the metrics are normalized, a negative $\mathcal{P}_i$ value indicates an improvement in mesh quality whereas a positive $\mathcal{P}_i$ value indicates a worsening of mesh quality. We also report the number of nodes moved during the mesh smoothing process, $C_S$, which corresponds to the number of calls made to each smoother. For the combined approach, $C_S$ is reported as the number of calls to the $\ell_2$ smoother plus the number of calls to the $\ell_{\text{inf}}$ smoother.

Table 2: Mesh quality improvement results for the optimization-based smoothing techniques

| Technique | $N_S$ ($\mathcal{P}$) | $\kappa_{avg}$ ($\mathcal{P}$) | $\kappa_{max}$ ($\mathcal{P}$) | $A_{\gamma_{avg}}$ ($\mathcal{P}$) | $A_{\gamma_{max}}$ ($\mathcal{P}$) | $C_S$ |
|---|---|---|---|---|---|---|
| Duct Geometry | | | | | | |
| Laplacian | 78 (+100) | – | – | 1.452 (+.76) | 24.25 (+367) | 1303 |
| Smart Lap. | 31 (-20.5) | 1.300 (-.38) | 3.691 (-2.6) | 1.433 (-.56) | 4.964 (4.3) | 732 |
| $\ell_2$ Opt. | 15 (-62) | 1.275 (-2.2) | 3.690 (-2.6) | 1.400 (-2.8) | 4.578 (-11.8) | 2773 |
| $\ell_{inf}$ Opt. | 4 (-90) | 1.379 (+5.7) | 3.045 (-19.7) | 1.571 (+9.0) | 3.979 (-23.3) | 5498 |
| Restricted $\ell_{inf}$ | 4 (-90) | 1.313 (+.61) | 3.045 (-19.7) | 1.493 (+3.6) | 3.979 (-23.3) | 32 |
| Combined | 4 (-90) | 1.280 (-2.2) | 3.045 (-19.7) | 1.409 (-2.2) | 3.980 (-23.3) | 2773+13 |
| Gear Geometry | | | | | | |
| Laplacian | 63 (+152) | – | – | 1.661 (+2.4) | 84.80 (+1673) | 1051 |
| Smart Lap. | 11 (-56) | 1.414 (-.63) | 3.309 (-4.0) | 1.610 (-.74) | 4.782 (0) | 492 |
| $\ell_2$ Opt. | 3 (-88) | 1.378 (-3.2) | 3.657 (+6.1) | 1.560 (-3.8) | 5.201 (+8.8) | 2141 |
| $\ell_{inf}$ Opt. | 0 (-100) | 1.455 (+2.2) | 2.996 (-13.1) | 1.682 (+3.6) | 3.703 (-22.5) | 2213 |
| Restricted $\ell_{inf}$ | 0 (-100) | 1.425 (+.14) | 2.996 (-13.1) | 1.627 (+.31) | 4.744 (-13.1) | 24 |
| Combined | 0 (-100) | 1.380 (-3.0) | 2.996 (-13.1) | 1.562 (-3.6) | 3.953 (-17.3) | 2141+3 |
| Hook Geometry | | | | | | |
| Laplacian | 64 (+113) | 1.393 (+2.4) | 74.28 (+1335) | 1.569 (+2.3) | 88.19 (+1334) | 1443 |
| Smart Lap. | 27 (-10) | 1.356 (-.25) | 5.176 (0) | 1.529 (-.26) | 6.151 (0) | 798 |
| $\ell_2$ Opt. | 7 (-77) | 1.331 (-2.1) | 3.747 (-27.6) | 1.495 (-2.4) | 4.437 (-27.9) | 2933 |
| $\ell_{inf}$ Opt. | 0 (-100) | 1.429 (+5.1) | 2.973 (-48.0) | 1.659 (+8.2) | 4.331 (-29.6) | 5970 |
| Restricted $\ell_{inf}$ | 0 (-100) | 1.367 (+.51) | 2.990 (-42.2) | 1.549 (+1.0) | 4.331 (-29.6) | 34 |
| Combined | 0 (-100) | 1.332 (-2.1) | 2.973 (-42.6) | 1.497 (-2.3) | 4.331 (-29.6) | 2933+5 |
| Foam Geometry | | | | | | |
| Laplacian | 82 (+74) | – | – | 1.622 (+2.7) | 83.17 (+914) | 916 |
| Smart Lap. | 42 (-11) | 1.390 (-.14) | 4.362 (0) | 1.575 (-.25) | 8.197 (0) | 555 |
| $\ell_2$ Opt. | 21 (-55) | 1.372 (-1.4) | 4.310 (-1.2) | 1.552 (-1.7) | 6.760 (-17.5) | 2637 |
| $\ell_{inf}$ Opt. | 25 (-47) | 1.447 (+4.0) | 4.310 (-1.2) | 1.672 (+5.8) | 6.596 (-19.5) | 3376 |
| Restricted $\ell_{inf}$ | 25 (-53) | 1.398 (+.43) | 4.310 (-1.2) | 1.590 (+.70) | 6.596 (-19.5) | 33 |
| Combined | 24 (-49) | 1.375 (-1.2) | 4.310 (-1.2) | 1.556 (-1.4) | 6.596 (-19.5) | 2637+11 |

In three of the four cases, Laplacian smoothing results in a mesh containing inverted elements. The CUBIT software defines the condition number of inverted elements to be $10^6$, which skews the $\kappa_{avg}$ and $\kappa_{max}$ values for those meshes; we do not report those results. In all four cases, Laplacian smoothing worsens mesh quality by every measure reported: the number of slivers is approximately doubled, $A_{\gamma_{avg}}$ increases by more than two percent, and $A_{\gamma_{max}}$ is significantly worsened in all four cases. By design, the "smart" Laplacian smoother improves the mesh in each case, but the improvement in the average element quality is less than .5 percent in all cases, and the improvement in the maximum quality values is zero in two of the four cases.

In contrast, the optimization-based smoothing approaches preserve mesh validity in all four test cases, and each approach significantly improves the mesh by some measure of mesh quality. Both the $\ell_2$ and $\ell_{inf}$ smoothers are able to eliminate a majority of the slivers. The $\ell_{inf}$ smoother typically does better than $\ell_2$ with respect to this metric, and in two of the four cases eliminates all of the slivers from the mesh. As expected, the $\ell_2$ smoother improves the average element quality in all four cases by as much 3.2 percent. Although it is not designed to improve $\kappa_{max}$, this can happen serendipitously as is evidenced in three of the four cases. In the gear geometry, however, $\kappa_{max}$ worsens by about 6 percent. The results for the $\ell_{inf}$ smoother are the inverse of the $\ell_2$ results. The average element quality is worsened in each case by as much as 5.7 percent in the duct geometry, but the $\kappa_{max}$ and $A_{\gamma_{max}}$ values are always significantly improved. The restricted $\ell_{inf}$ smoother achieves nearly the same improvement in $\kappa_{max}$ and $A_{\gamma_{max}}$ as the $\ell_{inf}$ smoother without the corresponding decrease in average element quality. The combined optimization approach achieves the best overall improvement in each of the four cases; all quality metrics are significantly improved in all test cases, and its use is recommended.

In each case the number of calls to the $\ell_2$ smoother is roughly equal to the number of vertices in the mesh; that is, each local submesh is visited approximately only once. In constrast the $\ell_{inf}$ smoother is called more times, indicating more grid point movement. This is supported by the fact that the average element quality changes approximately twice as much when the $\ell_{inf}$ smoother is called significantly more times than the $\ell_2$ smoother. The restricted $\ell_{inf}$ smoother is called approximately once for each sliver in the mesh when used alone, and far fewer times when used in conjunction with the $\ell_2$ smoother. Currently the $\ell_{inf}$ and $\ell_2$ smoothers are about ten and one hundred times more expensive than smart Laplacian, respectively, and work to reduce computational cost is under way.

### 4.2 Mesh Untangling and Improvement

To demonstrate the effectiveness of optimization-based untangling, we used a randomized smoothing scheme on the original meshes given in Table 1 to create "tangled" meshes with valid connectivity but several hundred inverted elements. In Table 3, we give the number of inverted elements, $N_I$, the number of sliver elements, $N_S$, as well as the quality metrics $\kappa_{avg}$, $\kappa_{max}$, $A_{\gamma_{avg}}$, and $A_{\gamma_{max}}$ for each of the four tangled meshes. The results of the untangling procedure described in Section 3 are reported for each geometry in the rows labeled "Untangle". In each case the optimization-based procedure successfully eliminates all of the inverted elements from the mesh, but, as expected, the resulting mesh quality is quite poor. We therefore follow the untangling procedure with the combined optimization approach described in the previous section. In each case, even though we are starting from a significantly worse-quality mesh, we obtain the nearly same final mesh quality as reported in Table 2.

## 5 Conclusions

Our results indicate that Laplacian smoothing can be detrimental to the quality of simplicial meshes on complex geometries, and we do not recommend its use. In contrast, the optimization approaches, particularly the combined $\ell_2$ and $\ell_{inf}$ smoothing technique, significantly improved the quality of each of the test cases. We showed that the behavior of the more commonly accepted aspect ratio shape measure was mirrored by the behavior of the condition number shape measure, and that the condition number shape measure is theoretically optimal.

Strategically combining different local mesh smoothing strategies is not a new idea; a number of researchers have combined Laplacian smoothing with their optimization-based approaches to achieve good quality meshes at a low computational cost [19, 7]. However, this is the first instance we are aware of in which two optimization strategies have been combined to improve both the average element quality and the extremal element quality. Although our results showed that these improvements can be achieved for a small incremental cost to the $\ell_2$ strategy, further work is needed to reduce the overall cost of the approach. Techniques that combine Laplacian smoothing with the combined technique presented here are under consideration.

## Acknowledgments

The work of the first author was supported by the Mathematical, Information, and Computational Sciences Division subprogram of the Office of Advanced Scientific Computing Research, U.S. Department of Energy, under Contract W-31-109-Eng-38. The work of the second author was supported by the Department of Energy's Mathematics, Information and Computational Sciences Program (SC-31) and was performed at Sandia National Laboratories. Sandia is a multiprogram laboratory operated by Sandia Corporation, a Lockheed Martin Company, for the United States Department of Energy under Contract DE-ACO4-94AL85000.

## References

[1] R. E. Bank and R. K. Smith. Mesh smoothing using a posteriori error estimates. *SIAM Journal on Numerical Analysis*, 34(3):979–997, June 1997.

[2] Randy Bank. *PLTMG: A Software Package for Solving Ellipitc Parital Differential Equations,*

Table 3: Mesh quality improvement results for the optimization-based smoothing techniques

| Technique | $N_I$ | $N_S$ | $\kappa_{avg}$ | $\kappa_{max}$ | $A_{\gamma_{avg}}$ | $A_{\gamma_{max}}$ | $C_U$ | $C_S$ |
|---|---|---|---|---|---|---|---|---|
| Duct Geometry | | | | | | | | |
| Tangle | 402 | 1049 | – | – | 6.321 | 72.09 | – | – |
| Untangle | 0 | 75 | 1.318 | 11.06 | 1.393 | 24.72 | 2068 | – |
| Combined | 0 | 4 | 1.281 | 3.045 | 1.409 | 3.980 | – | 2954+14 |
| Gear Geometry | | | | | | | | |
| Tangle | 297 | 764 | – | – | 20.63 | $3.95^4$ | – | – |
| Untangle | 0 | 56 | 1.477 | 89.24 | 1.688 | 125.9 | 1785 | – |
| Combined | 0 | 0 | 1.380 | 2.996 | 1.562 | 3.809 | – | 2305+3 |
| Hook Geometry | | | | | | | | |
| Tangle | 515 | 1252 | – | – | 7.559 | $2.43^3$ | – | – |
| Untangle | 0 | 58 | 1.381 | 38.86 | 1.558 | 45.91 | 2557 | – |
| Combined | 0 | 0 | 1.332 | 2.973 | 1.497 | 4.331 | – | 3160+5 |
| Foam Geometry | | | | | | | | |
| Tangle | 299 | 828 | – | – | 4.419 | $1.07^3$ | – | – |
| Untangle | 0 | 82 | 1.419 | 49.91 | 1.609 | 60.17 | 1580 | – |
| Combined | 0 | 24 | 1.375 | 4.310 | 1.555 | 6.709 | – | 2760+11 |


*Users' Guide 7.0*, volume 15 of *Frontiers in Applied Mathematics*. SIAM, Philadelphia, 1994.

[3] J. Demmel. *Applied Numerical Linear Algebra*. SIAM, Philadelphia, Pennsylvania, 1997.

[4] J. Dompierre, P. Labbe, F. Guibault, and R. Camerero. Proposal of benchmarks for 3d unstructured tetrahedral mesh optimization. In *Proceedings of the 7th International Meshing RoundTable'98*, pages 459–478, 1998.

[5] T. D. Blacker et. al. CUBIT mesh generation environment. Technical Report SAND94-1100, Sandia National Laboratories, Albuquerque, New Mexico, May 1994.

[6] David A. Field. Laplacian smoothing and Delaunay triangulations. *Communications and Applied Numerical Methods*, 4:709–712, 1988.

[7] Lori Freitag. On combining Laplacian and optimization-based smoothing techniques. In *Trends in Unstructured Mesh Generation*, volume AMD-Vol. 220, pages 37–44. ASME Applied Mechanics Division, 1997.

[8] Lori Freitag. Users manual for Opt-MS: Local methods for simplicial mesh smoothing and untangling. Technical Report ANL/MCS-TM-239, Mathematics and Computer Science Division, Argonne National Laboratory, Argonne, Ill., 1999.

[9] Lori Freitag and Carl Ollivier-Gooch. A comparison of tetrahedral mesh improvement techniques. In *Proceedings of the Fifth International Meshing Roundtable*, pages 87–100. Sandia National Laboratories, 1996.

[10] Lori Freitag and Paul Plassmann. Local optimization-based simplicial mesh untangling and improvement. Preprint ANL/MCS-P749-0399, Mathematics and Computer Science Division, Argonne National Laboratory, Argonne, Ill., August, 1999.

[11] Lori A. Freitag, Mark T. Jones, and Paul E. Plassmann. An efficient parallel algorithm for mesh smoothing. In *Proceedings of the Fourth International Meshing Roundtable*, pages 47–58. Sandia National Laboratories, 1995.

[12] P. L. George and H. Borouchaki. *Delaunay Triangulation and Meshing*. Hermes, Paris, 1998.

[13] Roger Horn and Charles Johnson. *Matrix Analysis*. Cambridge University Press, Cambridge, 1986.

[14] Patrick Knupp. Achieving finite element mesh quality via optimization of the Jacobian matrix norm and associated quantities, Part I - A framework for surface mesh optimization. Technical Report SAND 99-0110J, Sandia National Laboratories, 1999.

[15] Patrick Knupp. Achieving finite element mesh quality via optimization of the Jacobian matrix norm and associated quantities, Part II - A framework for volume mesh optimization. Technical Report SAND 99-0709J, Sandia National Laboratories, 1999.

[16] S. H. Lo. A new mesh generation scheme for arbitrary planar domains. *International Journal for Numerical Methods in Engineering*, 21:1403–1426, 1985.

[17] V. N. Parthasarathy, C. M. Graichen, and A. F. Hathaway. A comparison of tetrahedron quality measures. *Finite Element Analysis and Design*, 15:255–261, 1993.

[18] Matthew L. Staten Scott A. Canann, Joseph R. Tristano. An approach to combined Laplacian and optimization-based smoothing for triangular, quadrilateral, and quad-dominant meshes. In *Proceedings of the 7th International Meshing Roundtable*, pages 479–494. Sandia National Laboratories, 1998.

[19] Mark Shephard and Marcel Georges. Automatic three-dimensional mesh generation by the finite octree technique. *International Journal for Numerical Methods in Engineering*, 32:709–749, 1991.